Internal tree cycling and atmospheric archiving of mercury: examination with concentration and stable isotope analyses.

David S. McLagan [1,2,3], Harald Biester[1], Tomas Navrátil[4], Stephan M. Kraemer[5], Lorenz Schwab[5,6]

[1]Institute of Geoecology, Technical University of Braunschweig, Braunschweig, 38106, Germany

[2]Dept. of Physical and Environmental Sciences, University of Toronto Scarborough, M1C1A4 Canada

[3]School of Environmental Studies and Dept. of Geological Sciences and Geological Engineering, Queen's University, K7L3N6 Canada

[4]Institute of Geology of the Czech Academy of Sciences, Prague, 117 20, Czech Republic

[5]Department for Environmental Geochemistry, Centre for Microbiology and Environmental Systems Science, University of Vienna, Vienna, 1090, Austria

[6]Doctoral School in Microbiology and Environmental Science, University of Vienna, Vienna, 1090, Austria

Correspondence to: david.mclagan@queensu.ca
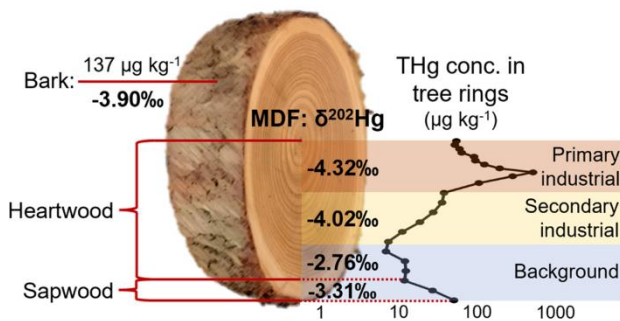
Abstract. Trees predominantly take up mercury (Hg) from the atmosphere via stomatal assimilation of gaseous elemental Hg (GEM). Hg is oxidised in leaves/needles and transported to other tree anatomy including bole wood where it can be stored long-term. Using Hg associated with growth rings facilitates archiving of historical GEM concentrations. Nonetheless, there are significant knowledge gaps on the cycling of Hg within trees. We investigate Hg archived in tree rings, internal tree Hg cycling, and differences in Hg uptake mechanisms in Norway spruce and European larch sampled within 1 km of a $HgCl_2$ contaminated site using total Hg (THg) and Hg stable isotope analyses. Tree ring samples are indicative of significant increases in THg concentrations (up to $521 \mu g \cdot kg^{-1}$) from *background period* (*BGP*; facility closed; 1992—present) to *secondary industrial period* (*$2^{nd}IP$*; no $HgCl_2$ wood treatment; 1962–1992) to *primary industrial period* (*$1^{st}IP$*; active $HgCl_2$ wood treatment; ≈1900–1962). Mass dependent fractionation (MDF) Hg stable isotope data are shifted negative during industrial periods (δ^{202}Hg: *$1^{st}IP$*: -4.32 ± 0.15‰; *$2^{nd}IP$*: -4.04 ± 0.32‰; *BGP:* -2.83 ± 0.74‰; 1SD). Even accounting for a ≈-2.6‰ MDF shift associated with stomatal uptake, these data are indicative of emissions derived from industrial activity being enriched in lighter isotopes associated with $HgCl_2$ reduction and Hg^0 volatilisation. Similar MDF (δ^{202}Hg: -3.90 ± 0.30‰; 1SD) in bark Hg ($137 ± 105 \mu g \cdot kg^{-1}$) suggests that stomatal assimilation and downward transport is also the dominant uptake mechanism for bark Hg (reflective of negative stomatal uptake MDF shift) rather than deposition to bark. THg was enriched in sapwood of all sampled trees across both tree species. This may indicate long-term storage of a fraction of Hg in sapwood or xylem solution. We also observed a small range of odd isotope-MIF. Differences in Δ^{199}Hg between periods of different industrial activities were

significant (Δ^{199}Hg: *1^{st}IP*: 0.00 ± 0.03 ‰; *2^{nd}IP*: -0.06 ± 0.04 ‰, *BGP*: -0.13 ± 0.03 ‰, 1SD), and we suggest MIF signatures are conserved during stomatal assimilation (reflect source MIF signatures). These data advance our understanding of the physiological processing of Hg within trees and provide critical direction to future research into the use of trees as archives for historical atmospheric Hg.

Key words

Mercury biogeochemistry, tree rings, sapwood (hydroactive xylem), heartwood, phloem, bark, process and source tracing.

1. Introduction

Until the last 10—15 years, it was hypothesised that the major transfer pathway of mercury (Hg) from the atmospheric to terrestrial and aquatic matrices was the wet and dry deposition of Hg(II) as either gaseous oxidised Hg (GOM) or particulate bound-Hg (PBM) (Lin and Pehkonen, 1999; Lindberg et al., 2007; Selin, 2009). However, studies began to suggest that dry deposition of gaseous elemental Hg (GEM) had to be more important than was thought because of inconsistencies between measurement data of atmospheric Hg species and modelling predictions (Selin et al., 2008; Zhang et al., 2009; Mao and Talbot, 2009). A major mechanism for dry deposition of GEM is uptake and assimilation to flora via stomata during plant respiration, an idea that was posited by scientists as far back as the late 1970s (Browne and Fang, 1978; Lindberg et al., 1979). The rate of GEM uptake correlates to photosynthetic activity of the plants (Laacouri et al., 2013), but is also species dependent since it is related to stomatal conductance and the number of stomata per leaf (Laacouri et al., 2013; Millhollen et al., 2006). Recent work has provided evidence that dry deposition of GEM to vegetation via stomatal uptake and subsequent transfer via leaf/needle senescence, abscission, and litterfall is likely to be the dominant mechanism for Hg deposition from the atmosphere to terrestrial matrices (Obrist et al., 2017; 2018; Jiskra et al., 2018).Similarly, there is strong evidence that GEM is also the major source of Hg in bole wood of trees (Scanlon et al, 2020, Wang et al., 2020; 2021). Using Hg stable isotope measurements, stomatal assimilation of GEM has been estimated to supply 57—94 % of total Hg (THg) in vegetated terrestrial systems (Khan et al., 2019 and references therein). A major loss mechanism of Hg from forest ecosystems is during biomass burning (Friedli et al., 2009; McLagan et al., 2021a; Dastoor et al., 2022).

To assess Hg cycling within trees we must also reflect on alterative uptake mechanisms: (i) uptake from roots and (ii) deposition to above ground tree surfaces (stems, leaves, and bark) and potential sorption to and translocation into tree tissue. Hg uptake from roots has been studied for decades. Data overwhelmingly show minimal transport of Hg from the root zone to aerial mass of trees (Beauford et al., 1977; Lindberg et al., 1979; Bishop et al., 1998; Moreno et al., 2005; Graydon et al. 2009; Cui et al., 2014; Cozzolino et al., 2016; Peckham et al., 2019a). Even in soils with elevated THg concentrations, upward transfer from roots is low in relative terms (Beauford et al., 1977; Lindberg et al., 1979; Graydon et al. 2009). Limited uptake of Hg and other metals via the roots has been attributed to restrictive barriers in the roots such as that provided by the endodermis (Kahle, 1993). Alternatively, Hg can also be deposited to surfaces of the aerial anatomy of trees, predominantly as GOM and PBM (Rea et al., 2002; Mowat et al., 2011; Laacouri et al., 2013). Hg on leaf surfaces contributes only a minor fraction of THg in foliage and accumulation rates are low due to both precipitation wash-off (Rea et al., 2000; 2001; Laccouri et al., 2013) and photoreduction and subsequent evasion of GEM (Graydon et al., 2006; Mowat et al., 2011). Several studies have demonstrated elevated bark THg concentrations relative to branch and bole wood (Siwik et al., 2010; Zhou et al., 2017; Liu et al., 2020). Therefore, it has been suggested that Hg in bark is chiefly derived from atmospheric deposition (Chiarantini et al., 2016; 2017) potentially with a greater proportion of GOM and PBM rather than GEM (Peckham et al., 2019a).

2

Trees make up a large sink for atmospheric Hg and therefore play an important role in the global Hg cycle. Hg has no known biological function in plants (Moreno-Jiménez et al., 2006; Peralta-Videa et al., 2009; Cozzolino et al., 2016); thus, it is important to understand the physiological processing of Hg within trees from a phytotoxicological standpoint. After assimilation through leaf/needle stoma GEM is assumed to be oxidised to form Hg(II) compounds and integrate with internal leaf tissue (Laacouri et a., 2013; Demers et al., 2013). A recent study examining three evergreen species used Hg stable isotopes to show that reduction and re-release can occur (Yuan et al., 2018). Although the bole wood of trees has lower THg concentrations than bark and needles/leaves in both deciduous and evergreen species (Navrátil et al., 2017; Zhou et al., 2017; Liu et al., 2020), the overall Hg loading of the tree is the reverse: wood carries the largest total mass of Hg due to much greater overall biomass (Liu et al., 2020).

Hg is transported from the foliage to bole wood via the phloem, which is the conduit for nutrient and photosynthetic product transfer from leaves/needles to the rest of the trees (Cutter and Guyette, 1993). Phloem (first layer of inner bark) lies between the cambium (tissue that promotes new xylem and phloem growth) and the cork and outer bark. Once oxidised to Hg(II) species in the leaves/needles, it likely associates with phytochelatin, cysteine compounds for phloem transport (O'Connor et al., 2019; Dennis et al., 2019). Phloem-to-xylem translocation (new xylem makes up sapwood and forms tree rings) is expected to occur throughout this downward transport (Arnold et al., 2018; Yanai et al., 2020; Nováková et al., 2021; 2022). This translocation likely proceeds via *rays*, parenchyma cells that radially connect xylem and phloem conductive tissues and mediate water and nutrient transport, tree growth, and biotic and abiotic stressors (Nagy et al., 2014; Pfautsch et al., 2015; Gustin et al., 2022). THg is expected to be preserved in the newly forming xylem tree rings; and hence, THg concentrations in tree rings have been used as a proxy for historical atmospheric GEM concentration (Siwik et al., 2010; Wright et al., 2014; Clackett et al., 2018). This includes identification of elevated GEM concentrations, past and present, associated with atmospheric Hg emissions from industrial activities located near sampled trees (Odabasi et al., 2016; Navrátil et al., 2017; Scanlon et al., 2020; Nováková et al., 2022). A potential caveat to this method of chronicling historical atmospheric GEM concentrations is the translocation of Hg between tree rings that has been reported in certain studies; tree ring concentrations do not reflect reported industrial activity (Nováková et al., 2021; Wang et al., 2021). However, there are a number of studies that demonstrate this inter-ring translocation does not significantly influence results; tree ring Hg concentrations reflect reported industrial (Clackett et al., 2018; Navrátil et al., 2018; Peckham et al., 2019b). Tree species may be a factor affecting inter-ring Hg translocation (Scanlon et al., 2020; Nováková et al., 2021).

Hg stable isotopes represent a powerful and relatively new technique that can provide information relating to the biogeochemical cycling history and potentially source information of sampled Hg (Bergquist and Bloom 2007; 2009). This premise assumes distinct "signature" ratios of different sources, and mass-dependant (MDF) and mass-independent (MIF) fractionations of the seven stable Hg isotopes that can be imparted by environmental transformation processes (Bergquist and Bloom 2007; 2009). Forest ecosystems are no exception to this. For instance, Hg stable isotopes added substantial evidence to the argument that GEM stomatal assimilation and eventual litterfall (or vegetation death) was the dominant mechanism for Hg deposition to soils in vegetated ecosystems (Wang et al., 2017; Jiskra et al., 2018; Yuan et al., 2018). Studies examining Hg stable isotopes in tree-rings are limited (Scanlon et al., 2020; Wang et al., 2021). Both studies associated differences in MIF (Δ^{199}Hg) with varying sources over time, but Wang et al. (2021) suggested there were limitations to this interpretation due to inter-ring translocation of Hg. They also attribute differences in MDF (δ^{202}Hg) with physiological differences (i.e., inter-ring translocation, stomatal conductance, and canopy dynamics), particularly as they relate to tree species, and environmental factors (i.e., soil conditions, slope, and winds) (Wang et al., 2021).

In this study, we examine THg concentrations and stable isotopes in two coniferous tree species, Norway spruce (*Picea abies*) and European larch (*Larix decidua*), surrounding a legacy Hg contaminated site in the German Black Forest. We aim to investigate if historical records of the industrial activities correlate with elevated THg concentrations in tree rings of sampled trees. There are no records of historical atmospheric Hg emissions or concentrations at this site, which was subject primarily to soil and water contamination (application of low-volatility $HgCl_2$ solution) rather than combustion emissions to the atmosphere. Thus, we compliment tree-ring data with deployments of GEM passive air samplers (PASs) at the site to assess atmospheric GEM conditions at the former industrial site past (tree rings) and present (PASs). Using Hg stable isotopes, we aim to examine potential source related variations in MDF and MIF across the tree ring records and physiological processes that may separate pools of Hg in the transport mechanism from atmosphere to foliage to phloem to tree-ring/bole wood. Additionally, we aim to investigate if deposition and sorption of Hg to tree bark is the dominant mechanism for bark Hg (isotopically distinct from bole wood).

2. Methods

2.1. Study site

The study area is in the High Black Forest (≈850 m a.s.l.) in Baden-Württemberg, Germany. Trees were sampled within a 1 km radius of a former kyanisation facility that treated timber with ≈0.66% $HgCl_2$ solution for preservation with substantial losses of this contaminated solution to soils, groundwater, and stream water (Eisele, 2004, Richard et al., 2016; McLagan et al., 2022). Although the trees were sampled within a 1 km radius of the contaminated site, all trees were outside, and upslope of the area directly affected by Hg contamination to soils and groundwater. The location of the sampled trees, former industrial buildings, wood drying areas, and passive sampling locations are shown in Fig. 1. The history of the industrial activities at the site can be divided into three distinct periods:

1. *Primary (first) industrial period (1stIP; 1892-1961):* Reports on this contaminated site describe the operation of the kyanisation facilities (wood treatment with 0.66 % $HgCl_2$) from 1892 until site owners went bankrupt in 1961 (Weis, 2020; Eisele, 2004; Schrenk and Hiester, 2007).
2. *Secondary industrial period (2ndIP; 1962-1992):* The site was acquired by another company and wood use and timber production as well as storage of timber treated with $HgCl_2$ is reported to have continued at the site until 1992 (Eisele, 2004; Schrenk and Hiester, 2007).
3. *Background period (BGP; 1992-present):* The site lay fallow between 1992 and 2002 before site remediation (2002—2004) and conversion of the area to a commercial space (Eisele, 2004; Schrenk and Hiester, 2007).

These three periods will be referred to throughout the study under the descriptors of *1stIP, 2ndIP*, and *BGP*, respectively.

2.2. Sampling and sample preparation

Bole wood (tree ring) samples were collected via two methods. The first was using a 450 mm long, 5.15 mm diameter increment borer (Haglöf Sweden). The tree core was sampled at breast height (≈1.2—1.5 m above ground). Whole tree core samples were placed in lab grade sampling straws and double zip-seal bags for transport back to the lab, immediately frozen at -20 °C upon return, subsequently freeze dried (-80 °C and 7 pa), and then stored at room temperature in conical centrifuge tubes until analysis. Spruce 1—3, Spruce BG, and Larch 1—3 were all sampled by this method. Samples processed by this method were counted for rings, cut with a lab scalpel, and weighed into nickel boats for analysis after being freeze-dried.

The second method involved the collection of freshly cut (collected on day of tree felling) tree slices or "cookies" (see TOC art; Section S1) from ≈0.5 m above the ground. A ≈50 mm slice was cut from the

4

165   middle of each tree cookie with a large table saw. Individual samples of aggregated tree rings were cut from
166   this slice with a plain edge chisel and all exposed sides we cut away and discarded. Samples were then
167   frozen and freeze dried, and then stored at room temperature in conical centrifuge tubes until analysis.
168   Spruce ISO4—6 were sampled by this method.

169   The number of tree rings (temporal resolution) in any given sample was typically 5 years but varied
170   somewhat with higher resolution in samples from some trees during $1^{st}IP$ and $2^{nd}IP$, and lower in some
171   samples from Spruce ISO trees that required higher THg concentrations per sample for Hg stable isotope
172   analyses. Care was taken to remove bark and phloem from wood, but there may have been instances where
173   some phloem remained attached to the newest tree ring sample. Bark was sampled from Spruce ISO4—6.
174   Bark from Spruce ISO4 and Spruce ISO5 were divided into inner and outer bark (estimated as the middle of
175   the bark) using a disposable scalpel. These bark samples were then frozen and freeze dried, and then stored
176   at room temperature in conical centrifuge tubes until analysis. Cleaning methods for equipment and surfaces
177   is detailed in Section S1. As these samples are from living (or freshly cut) trees and not sampled on an
178   annual temporal resolution (there were multiple tree rings in each sample) no cross dating methods were
179   necessary; ring counting represents the most accurate method of dating. Sapwood was visually identified by
180   colour changes (Bertaud and Holmbom, 2004). However, any uncertainty associated with identification of
181   the exact number of sapwood rings is of little consequence to the study as the greatest THg enrichment in
182   sapwood was in the youngest tree rings, which, we can state with certainty, were sapwood rings.

2.3. Total Hg analyses

184   THg concentration of samples collected with the increment borer were made using a thermal desorption,
185   amalgamation and atomic adsorption spectrometry (DMA80, Milestone Instruments). Samples were counted
186   for rings, cut with a lab scalpel (see borer cleaning methods), weighed into nickel boats and then combusted
187   at 750 °C for 300 seconds. Reference materials, Apple leaves (SRM 1515, NIST) and China Soil (NCS-
188   DC73030; China National Analysis Centre for Iron and Steel), were measured throughout the analyses and
189   the recoveries were 103 ± 3 % ($n = 30$) and 99 ± 5 % ($n = 11$), respectively. Details of the GEM passive air
190   sampler methods and data can be found in Section S2. THg concentration for the ISO trees were calculated
191   from the analysis of traps after the pre-concentration for isotope analysis (DMA-80L). All samples were
192   considered on a dry-weight basis (after freeze-drying) to remove any potential bias associated with moisture
193   loss during transport and storage before freezing.

2.4. Hg stable isotope analyses

195   Hg stable isotope analyses were performed on tree slice samples from trees: Spruce ISO4—6. No larch trees
196   could be analysed for Hg stable isotopes as no larch tree slices could be collected. The low THg
197   concentration in many sections of the wood is a challenge for Hg stable isotope analyses. Low concentration
198   samples required pre-concentration and trapping by combusting samples in a DMA80 and then purging the
199   released Hg from multiple boats of the same sample into 5 mL traps consisting of 40 % (v/v) inverse aqua
200   regia that replaced HCl with BrCl. Further method details and quality control/assurance of these analyses are
201   provided in Section S4 (see also McLagan et al. (2022)). Traps with insufficient concentrations for isotope
202   analysis were pool using the purge and trap method detailed in Section S5. Hg stable isotope measurements
203   were made using a Nu Plasma II (Nu Instruments) inductively coupled plasma mass spectrometer (MC-ICP-
204   MS) connected to an HGX-200 cold vapour generator for Hg introduction (Teledyne Cetac) and a
205   desolvating nebulizer for external mass bias correction by Tl doping using NIST-997 (Aridus 2, Teledyne
206   Cetac) following a method previously established in our laboratory (see McLagan et al. (2022) and
207   Wiederhold et al. (2010) for method details). All samples and standards were diluted to match concentrations
208   within each session and samples were measured using standard bracketing with NIST-3133. Analytical
209   precision (2SD) and accuracy (using repeated measurements of "in-house" *ETH Fluka* standard standard) for

these analyses are reported in Section S6 along with full Hg stable isotope datasets. Isotope ratios are
reported as the deviation from the isotopic composition of the NIST-3133 standard using delta notation and
expressed in per mil (‰) (details in Section S4).

3. Results and Discussion

3.1. Elevated tree ring total Hg concentrations during industrial activity

Elevated THg concentrations were observed in both Norway Spruce (*P. abies*) and European larch (*L. decidua*) tree rings dated before the mid-1990s compared to tree rings from the background Norway spruce (Spruce BG), which was situated ≈5.5km west (upwind based on dominant westerly winds in the area) of the former industrial facility (Fig. 2; THg data in Section S4). These species were chosen due to suggested suitability for Hg archiving in previous studies (Hojdová et al., 2011; Nováková et al., 2021) and there was a distinct pattern in tree ring THg concentrations in across all sampled trees near the legacy contaminated site regardless of species. This resulted in four distinct periods: (i) slightly elevated THg concentration in sapwood (hydroactive xylem) rings (0—5, 0—10, or 0—15 year tree rings; see Section 3.3.2 for discussion), (ii) low THg concentration in rings from the *BGP* not influenced by any known industrial activity (1992—sapwood), (iii) increasing THg concentrations in rings from what we term the *2ndIP* (1962—1992), and (iv) very elevated THg concentrations during the active kyanising or *1stIP* (before 1962) (Fig. 2). Not all sampled trees were of sufficient age to cover all of these periods (no larch trees reached the *1stIP*), but all trees that were old enough did follow this trend albeit with some distinct inter-tree differences in THg concentrations (Fig. 2).

The THg concentrations ranged from ≈1—10 $\mu g \cdot kg^{-1}$ in heartwood tree rings from the *BGP*, and up to 521 $\mu g \cdot kg^{-1}$ in a sample dated from 1951—1953 during the *1stIP* in Spruce 1, which is ≈400—500 m northeast of the former kyanisation building and wood drying areas. Additionally, THg concentrations of up to 211 $\mu g \cdot kg^{-1}$ were measured in a sample dated 1974—1976 (*2ndIP*) in Spruce 2, which was the closest tree sampled to the former facility (≈200—300 m south). However, this tree was planted after the *1stIP*. Distance of the tree from the industrial source was a definite factor in the between tree variability in THg concentrations, which has also been documented by Navrátil et al. (2017) and Nováková et al. (2022). These THg concentrations are comparable to other studies with the high THg concentrations measured in tree rings such as Becnel et al. (2004) (Loblolly Pine and Red Maple; THg concentrations up to 644 $\mu g \cdot kg^{-1}$), Abreu et al. (2008) (Black Poplar; THg concentrations up to 280 $\mu g \cdot kg^{-1}$), and Nováková et al. (2022) (European larch; THg concentrations up to 249 $\mu g \cdot kg^{-1}$). However, the THg concentrations in our study are lower than the very high concentrations measured by Wang et al. (2021) (Masson Pine; THg concentrations up to 2140 $\mu g \cdot kg^{-1}$), which is likely associated with the source being a former Hg mine known to have emitted large quantities of elemental Hg (Hg(0)) to the atmosphere.

The THg concentrations in the tree rings generally provide a good representation of the industrial history of the site based on the applied ≈5-year sampling resolution. While the end of the *2ndIP* falls in the middle of the 25—30 year tree ring samples, there is an increase in THg concentrations in all trees in samples 30—35 year and greater (before 1990). This is most apparent in the Spruce 1 and Spruce 2, which are the two sampled spruce trees closest to the former kyanisation building and wood drying sites. The average THg concentration for Spruce 1 and Spruce 2 was significantly higher ($p = 0.031$ and $p < 0.001$, respectively) during the *2ndIP* (1962—1990; Spruce 1: 23.1 ± 12.8 $\mu g \cdot kg^{-1}$; and Spruce 2: 134 ± 56 $\mu g \cdot kg^{-1}$) than during the *BGP* (1990—sapwood; Spruce 1: 10.8 ± 2.6 $\mu g \cdot kg^{-1}$; and Spruce 2: 9.46 ± 3.65 $\mu g \cdot kg^{-1}$). There was a sharp increase in THg concentration in the closest larch tree to the site (Larch 1) at this time, but the tree only dated to 1978, which is less than halfway through the *2ndIP*. Spruce 1 was also indicative of significantly higher ($p = 0.007$) THg concentrations during the *1stIP* (150 ± 141 $\mu g \cdot kg^{-1}$) compared to the elevated THg concentrations of the *2ndIP*. These agrees with other studies that have demonstrated good

6

correlations between industrial activity and tree ring Hg (Clackett et al., 2018; Navrátil et al., 2017; 2018; Nováková et al. 2022). Nonetheless, several studies have suggested that Hg can translocate across tree rings, which results in temporal differences between tree ring Hg and reported industrial activities/inventories (Nováková et al., 2021; Wang et al., 2021). This should continue to be monitored closely in future studies, particularly considering the sapwood enrichment discussed in Section 3.3.2.

Although the exact location of the three Spruce ISO trees (tree slices collected for Hg stable isotope analysis) is unknown, they were from a deforested stand of spruce between 200—500 m further from the wood drying site than Spruce 1 on an easterly facing slope (away from the site). Consequently, the mean THg concentrations in the Spruce ISO4—6 were generally lower than in Spruce 1. Nonetheless, the same trends were observable: mean THg concentrations during the active industrial period (before 1962, THg: 44.2 $\pm$ 15.5 µg·kg^{-1}) were significantly greater ($p = 0.006$) than during the $2^{nd}IP$ (1962—1990, THg: 26.7 $\pm$ 15.7 µg·kg^{-1}), which were significantly greater ($p = 0.001$) than rings from 1990—sapwood (THg: 6.5 $\pm$ 4.6 µg·kg^{-1}) based on combined data from all three Spruce ISO trees.

3.2. Isotopically fractionated Hg in tree rings associated with industrial emissions

3.2.1. Mass dependant fractionation (MDF)

The THg concentration data from tree rings suggest substantial emissions of Hg to the atmosphere during the industrial period. However, the original Hg contamination at these sites was the treatment of timber with $HgCl_2$ solution, a species that has a high solubility and low volatility compared to Hg(0) (Henry's Law constant: Hg(0): $1.4x10^{-3}$ mol·m^{-3}·Pa^{-1}; $HgCl_2$: $2.7x10^4$ mol·m^{-3}·Pa^{-1}; Schroeder and Munthe, 1998). Thus, the majority of any Hg releases to the atmosphere must have occurred via reduction of Hg(II) to Hg(0) and subsequent volatilisation as GEM. Kinetic processes such as reduction and evaporation result in the product (Hg released to the atmosphere in this case) becoming enriched in lighter isotopes (more negative δ^{202}Hg; Bergquist and Blum, 2007; 2009). Like the THg concentrations, MDF values reflect a chronological trend: δ^{202}Hg values from the $1^{st}IP$ (δ^{202}Hg: -4.32 $\pm$ 0.15 ‰, 1SD) were significantly more negative ($p = 0.007$) than during the $2^{nd}IP$ (δ^{202}Hg: -4.02 $\pm$ 0.31 ‰; 1SD), which in turn were significantly more negative ($p < 0.001$) than rings from the BGP (δ^{202}Hg: -2.76 $\pm$ 0.76 ‰, 1SD; sapwood 0–5 year samples not included, see Section 3.3.2) based on combined data from all three Spruce ISO trees (Fig. 3A). Wang et al. (2021) observed similar, although weaker, trends in Masson pines near Hg contaminated sites in China (range: -5.06 ‰ to -2.53 ‰; median: -3.74 ‰). MDF (δ^{202}Hg) has also been examined in oak (-1.82 $\pm$ 0.09 ‰) and pitch pine (-2.98 $\pm$ 0.76 ‰; North America; Scanlon et al., 2020), conifers (-2.76 $\pm$ 0.46 ‰; China; Liu et al., 2021), evergreen trees (-3.15 $\pm$ 0.22 ‰; China; Wang et al., 2020), and harvested one-year old Norway spruce saplings (-2.71 $\pm$ 0.27 ‰; Germany; Yamakawa et al., 2021). δ^{202}Hg values in these studies were more similar to samples from the BGP in our study, which likely relates to their low bole wood THg concentrations associated with the remoteness of their study sites from contamination sources (Scanlon et al., 2020; Wang et al., 2020; Liu et al., 2021; Yamakawa et al., 2021).

McLagan et al. (2022) highlight the difficulties in characterising a specific source signature of Hg stocks used in industrial activities due to the variability in stock δ^{202}Hg values, potential change in Hg supplies during the facility's lifetime, and the possibility that the industrial use of Hg resulted in the Hg emitted to different environmental media being fractionated from the original Hg stock. The highly negative δ^{202}Hg values during both the $1^{st}IP$ and $2^{nd}IP$ support the hypothesis that there was significant loss of Hg to the atmosphere during the industrial activities, which would result in the residual $HgCl_2$ in solution (major source of soil-groundwater contamination) being isotopically heavier than the original Hg stocks used at the site. Indeed, solid phase materials (listed as "SCA1" and "TSA" in McLagan et al., 2022) beneath the former kyanisation plant with THg concentrations >50 µg·kg^{-1} had mean δ^{202}Hg values of 0.06 $\pm$ 0.23 ‰ (McLagan

300 et al., 2022). This is at the positive end of the range of δ^{202}Hg values reported for cinnabar ores and
301 commercial liquid Hg^0 stocks (Sun et al., 2016; Grigg et al., 2018).

302 δ^{202}Hg for GEM in background air is typically in the range of $\approx$-0.2 to 1.5 ‰ (Szponar et al., 2020 and
303 references therein). Foliar uptake of GEM is reported to cause substantial MDF of between -2.3 and -2.9 ‰
304 (Demers et al., 2013; Enrico et al., 2016; Wang et al., 2021). If we subtract the middle of the estimated range
305 of MDF caused by foliar uptake (δ^{202}Hg: -2.6 ± 0.3 ‰) from the mean δ^{202}Hg values measured in tree rings
306 during *1stIP* and *2ndIP* we get δ^{202}Hg estimates of -1.7 ± 0.2 ‰ and -1.4 ± 0.2 ‰ (propagated uncertainty),
307 respectively, for GEM during these periods at the approximate location of the southeast facing forest stand
308 where the Spruce ISO trees were sampled (see also Fig. 4). This agrees with other studies that suggest
309 industrial sources of Hg are enriched in lighter isotopes compared to background air (Jiskra et al., 2019;
310 Szponar et al., 2020, and references therein). These estimates assume Hg in tree rings is derived from foliar
311 uptake of GEM from the atmosphere, which is suggested to be the dominant uptake pathway of Hg in trees
312 (e.g., Beauford et al., 1977; Graydon et al. 2009; Cozzolino et al., 2016), and no further MDF during
313 downward transport of Hg within the trees (as observed by Liu et al., 2021).

314 Applying the same correction to the δ^{202}Hg in tree rings from the *BGP* we get a δ^{202}Hg estimate of -0.2 ± 0.3
315 ‰ for GEM during this time (see also Fig. 4). This is right on the lower end of the reported range for δ^{202}Hg
316 of typical background GEM and suggests there may still be some minor inputs of Hg from the still
317 contaminated soils (McLagan et al., 2022) to the trees during the *BGP*. GEM concentrations were measured
318 with PASs over the areas of the former kyanisation building and wood drying areas (2.9 ± 0.6 ng·m^{-3}) and
319 concentrations were approximately double typical European background concentrations ($\approx$1.5—2.0 ng·m^{-3})
320 (Sprovieri et al., 2016). Other studies that have observed more elevated GEM concentrations with co-located
321 GEM PAS deployments: up to three orders of magnitude higher concentrations at a former Hg mine
322 (McLagan et al., 2018) and 3—4x higher at a Hg contaminated waste site (McLagan et al., 2021b).
323 Therefore, we can assume the slightly elevated GEM concentrations detected at the site in 2018 are
324 associated with low-level GEM emission from the site. These minor emissions likely cause a small negative
325 shift in δ^{202}Hg values of the tree rings from what might be expected of "true" background values. To our
326 knowledge this is the first study to address elevated GEM concentrations from a former Hg kyanisation
327 facility.

3.2.2. Mass independent fractionation (MIF)

329 We also observed small variability in odd isotope-MIF in the Spruce ISO tree rings (Fig. 3B). The mean
330 Δ^{199}Hg for the *1stIP* (Δ^{199}Hg: 0.00 ± 0.03 ‰, 1SD) was significantly greater ($p < 0.001$) than for the *2ndIP*
331 (Δ^{199}Hg: -0.06 ± 0.04 ‰, 1SD), which in turn was significantly greater ($p < 0.001$) than the *BGP* (Δ^{199}Hg: -
332 0.13 ± 0.03 ‰, 1SD). The Δ^{199}Hg of the *1stIP* is right at the mean values for cinnabar ores (Δ^{199}Hg: 0.01 ±
333 0.10 ‰, 1SD) and liquid Hg(0) stocks (Δ^{199}Hg: -0.01 ± 0.03 ‰, 1SD) (Sun et al., 2016; Grigg et al., 2018).
334 Additionally, the mean Δ^{199}Hg values from the solid phase materials at this contaminated site
335 were -0.01 ± 0.06 ‰ (McLagan et al., 2022). Hence, we suggest Δ^{199}Hg values in the tree rings during *1stIP*
336 are conserved from the industrial activities.

337 Wang et al. (2021) made similar observations in Masson Pine tree rings near a former Hg mine in Guizhou
338 Province of China: more positive Δ^{199}Hg values during periods of more intense industrial activity. The more
339 negative Δ^{199}Hg values in tree rings from the *BGP* are similar to the more negative background GEM values
340 (typical range: -0.4 to 0.0 ‰; Szponar et al., 2020 and references therein). Scanlon et al. (2020) measured
341 low THg concentration (<4.5 µg·kg^{-1}) in red oak, white oak, and pitch pine tree rings and negative Δ^{199}Hg
342 values (-0.39 to -0.14 ‰) and also associated this with the characteristic GEM signature of background air.
343 The difference in Δ^{199}Hg between the *1stIP, 2ndIP*, and *BGP* is likely related to the atmospheric mixing of
344 background GEM with industrially derived Hg. Foliar uptake has been reported to impart a small negative

Δ^{199}Hg shift (≈-0.1 to -0.2 ‰; Demers et al., 2013; Yuan et al., 2018). Yet, our data were more indicative of sources (industrial or background); thus, any negative Δ^{199}Hg shift may be small in Norway spruce and/or differences fall within the range of variability of the sources.

Information on the specific processes driving odd-MIF (nuclear volume effect (NVE) vs magnetic isotope effect (MIE)) in the measured Hg can be derived from the ratio of Δ^{199}Hg to Δ^{201}Hg (Bergquist and Blum, 2007; Blum et al., 2014). We derived a slope of 1.25 ± 0.13 (1SE) for bole wood using York orthogonal regression (Fig. S8.1; York et al., 2004), which is higher than other studies (1.04 in Wang et al., 2021; and 1.05 in Scanlon et al., 2020 and Liu et al., 2021), but still lies in the range of the expected slope (1.0—1.3) for MIE related photochemical reduction of Hg(II) to Hg(0) (Bergquist and Blum, 2007; Zheng et al., 2009). The observed MIF data suggest MIE related photochemical reduction and subsequent Hg(0) evasion is likely the dominant pathway of Hg(0) to the atmosphere. However, we caution against the over interpretation of these data as there was a large difference in the slope using a different orthogonal regression method (Fig. S8.1; Deming 1943). This difference in methods can largely be explained by the limited extent of odd-MIF observed in the tree ring data.

Both, Δ^{200}Hg and Δ^{204}Hg values show there was no significant even isotope-MIF in the bole wood samples (Section S8). Δ^{200}Hg anomalies have been reported for Hg in precipitation samples and related to upper atmosphere oxidation of Hg(0) (Gratz et al., 2010; Chen et al., 2012). Thus, the near zero even-MIF supports the hypothesis that the Hg in tree rings relates to foliar uptake of atmospheric GEM (unaffected by even-MIF) rather than root uptake of Hg deposited to soils via wet deposition of Hg(II).

3.3. Physiological and species related factors impacting within tree Hg cycling

3.3.1. THg concentration and stable Hg isotopes in bark

THg concentrations in the bark of three Spruce ISO trees (137 ± 105 µg·kg^{-1}) were significantly higher than THg in bole wood of *BGP* ($p = 0.014$), *2ndIP* ($p = 0.025$), and *1stIP* ($p = 0.042$). Furthermore, the bark was divided into inner (younger) and outer (older) bark of Spruce ISO4 and ISO5 trees and the outer bark was 2.0 and 2.7x higher in THg concentrations, respectively. This is similar to the observations made by Chiarantini et al. (2016) for black pine and could be related to longer and more exposure of the outer bark to elevated atmospheric Hg concentrations leading to more Hg deposited to these layers. Nonetheless, the older, outer bark would have been closer to the phloem (inner most bark layer; likely pathway for downward transport of Hg in trees) during the *1stIP* and *2ndIP* when we expect GEM concentrations were much higher than they are presently. Moreover, the inner bark concentrations (Spruce ISO4: 57.7 µg·kg^{-1}; Spruce ISO5: 163.1 µg·kg^{-1}) were still elevated with reference to the *BGP* in particular. Arnold et al. (2018) and Peckham et al. (2019a) suggest that translocation of Hg from the phloem into the inactive inner bark layers may be an important source of Hg stored within bark, which they further suggest supports findings by Chiarantini et al. (2016) that inner bark layers have a higher proportion of "organic Hg" than the outer layers in black pine.

If the predominant source of Hg in bark was via deposition of either GEM or GOM/PBM then we would expect to observe more positive δ^{202}Hg values in the bark samples as this pathway is unaffected by the large negative MDF (≈-2.6 ‰) associated with stomatal uptake. However, the δ^{202}Hg values for the bark samples were all highly negative (δ^{202}Hg: -3.90 ± 0.30 ‰, 1SD) and similar to the highly negative values in tree ring samples from the *1stIP* and *2ndIP*. Furthermore, GOM/PBM is reported to have more positive Δ^{199}Hg values than GEM (Szponar et al., 2020), but the bark samples (Δ^{199}Hg: -0.14 ± 0.06 ‰, 1SD) were similar if not slightly more negative than the bole wood from these industrial periods (Fig. 4). There was very little difference in δ^{202}Hg or Δ^{199}Hg between the inner and outer bark of either Spruce ISO4 or ISO5 tree (Table S4.1). In summary, our Hg stable isotope data suggests the stomatal uptake, internal transport, and translocation from phloem to inner bark is likely the dominant uptake pathway for Hg stored in bark. Liu et

389 al. (2021) posited the same foliage assimilation pathway for bark Hg uptake based on similar δ^{202}Hg and

390 Δ^{199}Hg values in both their bark and bole wood samples from subtropical evergreen species at a background

391 site. Considering *rays* that connect xylem and phloem reach as far as the inner bark (Nagy et al., 2014;

392 Pfautsch et al., 2015), this mechanism of bark Hg enrichment is a distinct possibility. More data across a

393 range of species, particularly using Hg stable isotopes, would be beneficial to determine the robustness of

394 this conclusion.

3.3.2. Sapwood (hydroactive xylem) rings enriched in Hg

396 THg concentrations were elevated in sapwood tree ring samples of all trees from both species, including

397 Spruce BG, compared to tree rings from the *BGP*. The 0—5 year samples were elevated in all trees and the

398 5—10 and 10—15 year samples were also higher in THg concentrations in some trees (Fig. 2). Although part

399 of the phloem may have been included in some 0—5 year samples and contributed to enrichment of these

400 samples, elevated THg concentrations in certain 5—10 and 10—15 year samples indicate this is not the sole

401 determinant. Sapwood enrichment has also been observed in both Norway spruce (Hojdová et al., 2011) and

402 European larch (Navrátil et al., 2018; Nováková et al., 2021; 2022) and various species of oak and pine

403 (Wright et al., 2014; Navrátil et al., 2017; Scanlon et al., 2020; Wang et al., 2021). Our study represents

404 perhaps the most pronounced and consistent (across all trees) example of this sapwood enrichment.

405 Nováková et al. (2021) suggest the tree coring sampling method could be a potential source of this

406 enrichment. However, we observe this in the Spruce ISO trees that were sampled by breaking up tree

407 "cookies" rather than coring, which would rule out this possibility.

408 We examine three alternate scenarios to explain this. The first is that GEM concentrations in the area have

409 been elevated during the last decade compared to the *BGP*. While the PAS measured GEM concentrations

410 were slightly elevated ($\approx$2x European background concentrations) likely associated with minor on-going

411 releases from contaminated topsoils, there is no evidence to suggest why GEM concentrations in the most

412 recent 5—10 years would be higher than the earlier *BGP*. Additionally, the Spruce BG tree also had elevated

413 THg concentrations in all samples under 15 years, which had little-to-no impact in tree ring Hg by the

414 industrial facility during $1^{st}IP$ or $2^{nd}IP$. The European Monitoring and Evaluation Programme (EMEP) has a

415 long-term monitoring station $\approx$22km to the west of the former industrial site ($\approx$16.5 km west of Spruce BG)

416 and reports a mean total gaseous Hg (predominantly GEM) concentration of 1.49 ng·m^{-3} ($\pm$0.24 ng·m^{-3}

417 measurement uncertainty; $\pm$ 0.12 ng·m^{-3} SD of annual means) over the last decade (EMEP, 2022), which is a

418 typical background concentration for Europe (Sprovieri et al., 2016). Hence, recently elevated GEM

419 concentrations cannot explain the elevated sapwood THg concentrations.

420 The second would relate to uptake of Hg from tree roots. The conductive or actively transporting component

421 of xylem (hydroactive xylem) exists within the sapwood of trees. Its primary role is the upward transport of

422 water and nutrients from tree roots to the aerial components and particularly leaves/needles. We have already

423 discussed how this pathway has been shown to be a minor mechanism of Hg uptake in many studies (e.g.,

424 Beauford et al., 1977; Graydon et al. 2009; Cozzolino et al., 2016). Also, the sampled trees are outside the

425 area in which surface contamination from the industrial activity occurred (particularly Spruce BG); any soil

426 contamination must have come from atmospheric Hg emissions and subsequent deposition, of which

427 stomatal uptake of GEM is the dominant conduit in forest ecosystems (Obrist et al., 2017; 2018; Jiskra et al.,

428 2018). We consider this mechanism highly unlikely to be driving sapwood enrichment.

429 The third scenario relates to tree physiology. Hg is transported downwards in trees via the phloem and has

430 been reported to translocate from phloem to xylem (sapwood) throughout this process (Arnold et al., 2018;

431 Yanai et al., 2020; Nováková et al., 2021). As sapwood ages it undergoes a physiological transition to

432 heartwood, which is drier, contains predominantly dead cells, and is used for structure rather than transport

433 (Bertaud and Holmbom, 2004; Metsä-Kortelainen et al., 2006). Hg that remains in the tree rings after the

10

transition to heartwood likely binds to components that endure this change, but there is a caveat in our knowledge of this process (Yanai et al., 2020; Nováková et al., 2021). Since we use dry weight THg concentrations, if all the Hg translocated from phloem to xylem was conserved in the wood during the transition from sapwood to heartwood, then we would not expect to see any sapwood enrichment. Thus, we deem it likely that some fraction of Hg is retained in the xylem solution or structures/chemicals enhanced in sapwood (compared to heartwood) of these species. Although we only have two samples from the 0—5 year tree rings analysed for stable isotopes, the δ^{202}Hg data from Spruce ISO5 and ISO6 are shifted negative (-0.41 and -0.33 ‰, respectively) in these samples compared to the adjacent composite sample of tree rings in each respective tree (Fig. 3A; Section S6). Hence, the process controlling retention of this Hg in sapwood would seem to favour lighter isotopes, implying there could be either preferential retention of specific Hg-compounds or a change in binding form during the retention process.

Any upwards transport of xylem solution Hg may contribute to the slightly elevated THg concentrations that Yanai et al. (2020) observed in tree rings at higher elevations above the ground. Sapwood is also a storage reserve for energy (starch) and water (Taylor et al., 2002); therefore, some of the Hg in xylem solution may be stored long-term in the hydroactive xylem without being transferred as the sapwood rings transition to heartwood. While long-term storage of some Hg in sapwood could be a factor driving temporal differences between tree ring THg concentrations and reported industrial activity in the literature (Arnold et al., 2018; Wang et al., 2021), our data do not reflect such Hg translocation. Ultimately, further research will be needed, particularly using Hg stable isotopes, to further explore this hypothesis and the physiological mechanisms behind this enrichment.

3.3.3. The impact of species on uptake and storage of Hg in tree rings

There is extensive discussion in the literature on species specific differences in THg concentrations of tree rings, particularly as they relate to foliar uptake rates (Wohlgemuth et al., 2020) and inter-ring translocation (Arnold et al., 2018; O'Connor et al., 2019). Inter-ring translocation has led some studies to question the overall effectiveness using tree rings as an archive for atmospheric GEM, but many of these studies have utilised oak (Scanlon et al., 2020), some pine species (Wang et al., 2021; Nováková et al., 2021), and Populus (Arnold et al., 2018). Certain physiological characteristics of these species (i.e., more radially conductive xylem) that enhance this translocation may limit their applicability to tree ring atmospheric archiving (Arnold et al., 2018; Nováková et al., 2021; Gustine et al., 2022). Several studies have observed strong correlations between THg concentrations in spruce (Hojdová et al., 2011) and larch (Navrátil et al., 2018; Nováková et al., 2021) tree rings and reported industrial activities and suggest these to be appropriate species for archiving atmospheric GEM concentrations.

Despite the quite apparent physiological differences between European larch (deciduous conifer) and Norway spruce (evergreen conifer), trends in THg concentrations varied little between the sampled trees of either species. Sapwood was enriched, *BGP* THg was low, and concentrations increased into the *2ndIP* at the same time (early 1990s) in both larch and spruce trees (all sampled larch were planted after the *1stIP*) (Fig. 2). Additionally, the good correlation between changes in THg concentrations and the timelines of the *1stIP*, *2ndIP*, and *BGP* suggest the process driving sapwood Hg enrichment results in limited inter-ring Hg translocation in Norway spruce and European larch; the fraction of Hg transferred to heartwood must be relatively consistent under this scenario. Thus, our data too suggest Norway spruce and European larch are effective species for the chronicling of historic GEM concentrations.

3.3.4. Between and within tree variability in tree ring Hg

Heterogeneity in the radial distribution of Hg has been observed in other studies and authors suggest sampling of multiple trees in each stand and different radial sections of trees provides more representative assessments (Wright et al., 2014; Peckham et al., 2019b). The sampling direction of the bole or height of the

11

sampling can cause differences within replicate samples from the same tree. Factors affecting between tree variability include microtopography, tree age or species and related specific physiological differences such as photosynthesis rate, stomatal conductance and transpiration (Binda et al., 2021). No correlation between Hg concentration and tree core mass was reported by Scanlon et al. (2020) and they concluded that differences in radial growth do not dilute or concentrate Hg in tree rings. These authors therefore concluded that Hg concentrations are a suitable proxy to evaluate trends of GEM. We detected some variability in THg concentrations between Spruce ISO4, ISO5, and ISO6 from the same stand of trees (Fig. 2) and in "replicated" tree rings from different sides of the Spruce ISO tree slices (mean relative difference: 78 ± 35 %; mean absolute difference: 5 ± 5 µg·kg^{-1}; $n = 10$; Table S3.1). Yet, variability in the ratios of Hg stable isotopes within the bole wood was low (mean absolute difference: δ^{202}Hg: 0.11 ± 0.08 ‰ 1SD; Δ^{199}Hg: 0.08 ± 0.02 ‰ 1SD; $n = 4$; Table S4.2). This suggests factors influencing radial Hg heterogeneity cause little impact of Hg stable isotopes. We considered the stable isotopes analyses based on combined data from all three trees, but individual trees also followed these trends (Section S6).

Data availability

All data are available within the paper and supplementary information. If there are any additional requests, please contact the authors.

Supplementary information

The Supporting Information is available free of charge at DOI: XXX.

Author Contribution

The project design and planning were made by DSM and LS, with inputs from TN. The manuscript was written predominantly by DSM with inputs from LS. Figures were prepared by DSM and LS. Supplemental information was prepared predominantly by LS with inputs from DSM. Tree core sampling was performed by DSM and LS, HB collected tree slices/"cookies". THg analyses were performed by LS and DSM, passive samplers were analysed by DSM, pre-concentration and isotope analysis was performed by LS. Lab space provided by HB and SMK. DSM, LS, HB, and TN contributed to manuscript reviews. DSM and LS contributed equally to this work.

Conflicts of Interest

The authors declare no competing financial interest.

Acknowledgements

References

Abreu, S. N., Soares, A. M. V. M., Nogueira, A. J. A., and Morgado, F.: Tree rings, Populus nigra L.; as mercury data logger in aquatic environments: Case study of an historically contaminated environment, Bull. Environ. Contam. Toxicol., 80(3), 294-299. DOI: 10.1007/s00128-008-9366-0, 2008.

Arnold, J., Gustin, M. S., and Weisberg, P. J.: Evidence for nonstomatal uptake of Hg by aspen and translocation of Hg from foliage to tree rings in Austrian pine, Environ. Sci Technol., 52(3), 1174-1182, DOI: 10.1021/acs.est.7b04468, 2018.

Beauford, W., Barber, J., and Barringer, A. R.: Uptake and distribution of mercury within higher plants, Physiol. Plant., 39(4), 261-265, DOI: 10.1111/j.1399-3054.1977.tb01880.x, 1977.

Becnel, J., Falgeust, C., Cavalier, T., Gauthreaux, K., Landry, F., Blanchard, M., Beck, M. J., and Beck, J.N.: Correlation of mercury concentrations in tree core and lichen samples in southeastern Louisiana, Microchem. J., 78(2), 205-210, DOI: 10.1016/j.microc.2004.06.002, 2004.

Bergquist, B. A., and Blum, J. D.: Mass-dependent and-independent fractionation of Hg isotopes by photoreduction in aquatic systems, Sci., 318(5849), 417-420, DOI: 10.1126/science.1148050, 2007.

Bergquist, B. A., and Blum, J. D.: The odds and evens of mercury isotopes: applications of mass-dependent and mass-independent isotope fractionation, Elements, 5(6), 353-357, DOI: 10.2113/gselements.5.6.353, 2009.

Bertaud, F., and Holmbom, B.: Chemical composition of earlywood and latewood in Norway spruce heartwood, sapwood and transition zone wood, Wood Sci. Technol., 38(4), 245-256, DOI: 10.1007/s00226-004-0241-9, 2004.

Binda, G., Di Lorio, A., and Monticelli, D.: The what, how, why, and when of dendrochemistry: (paleo)environmental information from the chemical analysis of tree rings, Sci. Tot. Environ., 758, 143672, DOI: 10.1016/j.scitotenv.2020.143672, 2021.

Bishop, K. H., Lee, Y. H., Munthe, J., and Dambrine, E.: Xylem sap as a pathway for total mercury and methylmercury transport from soils to tree canopy in the boreal forest, Biogeochem., 40(2), 101-113, DOI: 10.1023/A:1005983932240, 1998.

Blum, J. D., Sherman, L. S., and Johnson, M. W.: Mercury isotopes in earth and environmental sciences, Annu. Rev. Earth Planet. Sci., 42, 249-269, DOI: 10.1146/annurev-earth-050212-124107, 2014.

Browne, C. L., and Fang, S. C.: Uptake of mercury vapor by wheat: an assimilation model, Plant Physiol., 61(3), 430-433, DOI: 10.1104/pp.61.3.430, 1978.

Chen, J., Hintelmann, H., Feng, X., and Dimock, B.: Unusual fractionation of both odd and even mercury isotopes in precipitation from Peterborough, ON, Canada, Geochim. Cosmochim. Acta, 90, 33-46, DOI: 10.1016/j.gca.2012.05.005, 2012.

Chiarantini, L., Rimondi, V., Benvenuti, M., Beutel, M. W., Costagliola, P., Gonnelli, C., Lattanzi, P., and Paolieri, M.: Black pine (Pinus nigra) barks as biomonitors of airborne mercury pollution, Sci. Total Environ., 569, 105-113, DOI: 10.1016/j.scitotenv.2016.06.029, 2016.

Chiarantini, L., Rimondi, V., Bardelli, F., Benvenuti, M., Cosio, C., Costagliola, P., Di Benedetto, F., Lattanzi, P., and Sarret, G.: Mercury speciation in Pinus nigra barks from Monte Amiata (Italy): An X-ray absorption spectroscopy study, Environ. Pollut., 227, 83-88, DOI: 10.1016/j.envpol.2017.04.038, 2017.

Clackett, S. P., Porter, T. J., and Lehnherr, I.: 400-year record of atmospheric mercury from tree-rings in Northwestern Canada, Environ. Sci Technol., 52(17), 9625-9633, DOI: 10.1021/acs.est.8b01824, 2018.

Cozzolino, V., De Martino, A., Nebbioso, A., Di Meo, V., Salluzzo, A., and Piccolo, A.: Plant tolerance to mercury in a contaminated soil is enhanced by the combined effects of humic matter addition and inoculation with arbuscular mycorrhizal fungi, Environ. Sci. Pollut. Res., 23(11), 11312-11322, DOI: 10.1007/s11356-

13

557 016-6337-6, 2016.

558 Cui, L., Feng, X., Lin, C. J., Wang, X., Meng, B., Wang, X., and Wang, H.: Accumulation and translocation
559 of 198Hg in four crop species, Environ. Toxicol. Chem., 33(2), 334-340, DOI: 10.1002/etc.2443, 2014.

560 Cutter, B. E., and Guyette, R. P.: Anatomical, chemical, and ecological factors affecting tree species choice
561 in dendrochemistry studies, J. Environ. Qual., 22(3), 611-619, DOI:
562 10.2134/jeq1993.00472425002200030028x, 1993.

563 Dastoor, A., Angot, H., Bieser, J., Christensen, J., Douglas, T., Heimbürger-Boavida,. L. E., Jiskra, M.,
564 Mason, R., McLagan, D. S., Obrist, D., Outridge, P., Petrova, M., Ryjkov, A., St. Pierre, K., Schartup, A.,
565 Soerensen, A., Travnikov, O., Toyota, K., Wilson, S., and Zdanowicz, C.: Arctic mercury cycling, Nat. Rev.
566 Earth Environ., 3, 270-286, DOI: 10.1038/s43017-022-00269-w, 2022.

567 Demers, J. D., Blum, J. D., and Zak, D. R.: Mercury isotopes in a forested ecosystem: Implications for air-
568 surface exchange dynamics and the global mercury cycle, Global Biogeochem. Cy., 27(1), 222-238, DOI:
569 10.1002/gbc.20021, 2013.

570 Deming, W. E.: Statistical adjustment of data. Wiley, New Jersey, USA, 1943.

571 Dennis, K. K., Uppal, K., Liu, K. H., Ma, C., Liang, B., Go, Y. M., and Jones, D. P.: Phytochelatin database:
572 a resource for phytochelatin complexes of nutritional and environmental metals, Database, 2019, baz083,
573 DOI: 10.1093/database/baz083, 2019.

574 Eisele, G.: Arbeitshilfe Absicherbarkeit von Risiken beim Flächenrecycling, Forschungsbericht FZKA-
575 BWPLUS, Landesanstalt für Umwelt Baden-Württemberg, Baden-Württemberg, Germany, 102.
576 https://pd.lubw.de/99447, 2004.

577 EMEP: Co-operative Programme for Monitoring and Evaluation of the Long-Range Transmissions of Air
578 Pollutants in Europe, European Monitoring and Evaluation Programme (EMEP), Kjeller, Norway.
579 https://projects.nilu.no/ccc/reports.html, accessed: Feb 09, 2022, 2022.

580 Enrico, M., Roux, G. L., Marusczak, N., Heimbürger, L. E., Claustres, A., Fu, X., Sun, R., and Sonke, J. E.:
581 Atmospheric mercury transfer to peat bogs dominated by gaseous elemental mercury dry deposition,
582 Environ. Sci Technol., 50(5), 2405-2412, DOI: 10.1021/acs.est.5b06058, 2016.

583 Friedli, H. R., Arellano, A. F., Cinnirella, S., and Pirrone, N.: Initial estimates of mercury emissions to the
584 atmosphere from global biomass burning, Environ. Sci Technol., 43(10), 3507-3513, DOI:
585 10.1021/es802703g, 2009.

586 Gratz, L. E., Keeler, G. J., Blum, J. D., and Sherman, L. S.: Isotopic composition and fractionation of
587 mercury in Great Lakes precipitation and ambient air, Environ. Sci Technol., 44(20), 7764-7770, DOI:
588 10.1021/es100383w, 2010.

589 Graydon, J. A., St. Louis, V. L., Hintelmann, H., Lindberg, S. E., Sandilands, K. A., Rudd, J. W., Kelly, C.
590 A., Tate, M. T., Krabbenhoft, D. P., and Lehnherr, I.: Investigation of uptake and retention of atmospheric
591 Hg (II) by boreal forest plants using stable Hg isotopes, Environ. Sci Technol., 2009, 43(13), 4960-4966,
592 DOI: 10.1021/es900357s, 2009.

593 Grigg, A. R., Kretzschmar, R., Gilli, R. S., and Wiederhold, J. G.: Mercury isotope signatures of digests and
594 sequential extracts from industrially contaminated soils and sediments. Sci. Total Environ., 2018, 636, 1344-
595 1354, DOI: 10.1016/j.scitotenv.2018.04.261, 2018.

596 Gustin, M. S., Ingle, B., and Dunham-Cheatham, S. M.: Further investigations into the use of tree rings as

597   archives of atmospheric mercury concentrations, Biogeochem., 158, 167-180, DOI: 10.1007/s10533-022-
598   00892-1, 2022.

599   Hojdová, M., Navrátil, T., Rohovec, J., Žák, K., Vaněk, A., Chrastný, V., Bače, R., and Svoboda, M.:
600   Changes in mercury deposition in a mining and smelting region as recorded in tree rings, Water Air Soil
601   Pollut., 216(1), 73-82, DOI: 10.1007/s11270-010-0515-9, 2011.

602   Jiskra, M., Wiederhold, J. G., Skyllberg, U., Kronberg, R. M., Hajdas, I., and Kretzschmar, R.: Mercury
603   deposition and re-emission pathways in boreal forest soils investigated with Hg isotope signatures, Environ.
604   Sci Technol., 49(12), 7188-7196, DOI: 10.1021/acs.est.5b00742, 2015.

605   Jiskra, M., Sonke, J. E., Obrist, D., Bieser, J., Ebinghaus, R., Myhre, C. L., Pfaffhuber, K. A., Wängberg, I.,
606   Kyllönen, K., Worthy, D., and Martin, L. G.: A vegetation control on seasonal variations in global
607   atmospheric mercury concentrations, Nature Geosci., 11(4), 244-250, DOI: 10.1038/s41561-018-0078-8,
608   2018.

609   Jiskra, M., Maruszczak, N., Leung, K. H., Hawkins, L., Prestbo, E., and Sonke, J. E.: Automated stable
610   isotope sampling of gaseous elemental mercury (ISO-GEM): Insights into GEM emissions from building
611   surfaces, Environ. Sci Technol., 53(8), 4346-4354, DOI: 10.1021/acs.est.8b06381, 2019.

612   Kahle, H.: Response of roots of trees to heavy metals, Environ. Exp. Bot., 33(1), 99–119, DOI:
613   10.1016/0098-8472(93)90059-o, 1993.

614   Khan, T. R., Obrist, D., Agnan, Y., Selin, N. E., and Perlinger, J. A.: Atmosphere-terrestrial exchange of
615   gaseous elemental mercury: parameterization improvement through direct comparison with measured
616   ecosystem fluxes, Environ. Sci. Process. Impacts, 21(10), 1699-1712, DOI: 10.1039/C9EM00341J, 2019.

617   Laacouri, A., Nater, E. A., and Kolka, R. K.: Distribution and uptake dynamics of mercury in leaves of
618   common deciduous tree species in Minnesota, USA, Environ. Sci Technol., 47(18), 10462-10470, DOI:
619   10.1021/es401357z, 2013.

620   Lin, C. J., and Pehkonen, S. O.: The chemistry of atmospheric mercury: a review, Atmos. Environ., 33(13),
621   2067-2079, DOI: 10.1016/S1352-2310(98)00387-2, 1999.

622   Lindberg, S. E., Jackson, D. R., Huckabee, J. W., Janzen, S. A., Levin, M. J., and Lund, J. R.: Atmospheric
623   emission and plant uptake of mercury from agricultural soils near the Almaden mercury mine, J. Environ.
624   Qual., 8(4), 572-578, DOI: 10.2134/jeq1979.00472425000800040026x, 1979.

625   Lindberg, S., Bullock, R., Ebinghaus, R., Engstrom, D., Feng, X., Fitzgerald, W., Pirrone, N., Prestbo, E.,
626   and Seigneur, C.: A synthesis of progress and uncertainties in attributing the sources of mercury in
627   deposition, Ambio, 36(1), 19-32, http://www.jstor.org/stable/4315781, 2007.

628   Liu, Y., Lin, C. J., Yuan, W., Lu, Z., and Feng, X.: Translocation and distribution of mercury in biomasses
629   from subtropical forest ecosystems: Evidence from stable mercury isotopes, Acta Geochim., 40(1), 42-50,
630   DOI: 10.1007/s11631-020-00441-3, 2021.

631   Mao, H., and Talbot, R.: Speciated mercury at marine, coastal, and inland sites in New England–Part 1:
632   Temporal variability, Atmos. Chem. Phys., 12(11), 5099-5112, DOI: 10.5194/acp-12-5099-2012, 2012.

633   McLagan, D. S., Monaci, F., Huang, H., Lei, Y. D., Mitchell, C. P. J., and Wania, F.: Characterization and
634   quantification of atmospheric mercury sources using passive air samplers. J. Geophy. Res. Atmos., 124(4),
635   2351-2362, DOI: 10.1029/2018JD029373, 2019.

636   McLagan, D. S., Stupple, G. W., Darlington, A., Hayden, K., and Steffen, A.: Where there is smoke there is

mercury: Assessing boreal forest fire mercury emissions using aircraft and highlighting uncertainties associated with upscaling emissions estimates, Atmos. Chem. Phys., 21(7), 5635-5653, DOI: 10.5194/acp-21-5635-2021, 2021a.

McLagan, D. S., Osterwalder, S., and Biester, H.: Temporal and spatial assessment of gaseous elemental mercury concentrations and emissions at contaminated sites using active and passive measurements, Environ. Res. Commun., 3(5), p.051004, DOI: 10.1088/2515-7620/abfe02/meta, 2021b.

McLagan, D. S., Schwab, L., Wiederhold, J. G., Chen, L., Pietrucha, J., Kraemer, S. M., and Biester, H.: Demystifying mercury geochemistry in contaminated soil–groundwater systems with complementary mercury stable isotope, concentration, and speciation analyses, Environ. Sci. Process. Impacts, DOI: 10.1039/D1EM00368B, 2022.

Metsä-Kortelainen, S., Antikainen, T., and Viitaniemi, P.: The water absorption of sapwood and heartwood of Scots pine and Norway spruce heat-treated at 170 C, 190 C, 210 C and 230 C, Holz als Roh-und Werkstoff, 64(3), 192-197, DOI: 10.1007/s00107-005-0063-y, 2006.

Millhollen, A. G., Gustin, M. S., and Obrist, D.: Foliar mercury accumulation and exchange for three tree species, Environ. Sci Technol., 40(19), 6001-6006, DOI: 10.1021/es0609194, 2006.

Moreno, F. N., Anderson, C. W., Stewart, R. B., Robinson, B. H., Ghomshei, M., and Meech, J. A.: Induced plant uptake and transport of mercury in the presence of sulphur-containing ligands and humic acid. New Phytol., 166(2), 445-454, DOI: 10.1111/j.1469-8137.2005.01361.x, 2005.

Moreno-Jiménez, E., Gamarra, R., Carpena-Ruiz, R. O., Millán, R., Peñalosa, J. M., and Esteban, E.: Mercury bioaccumulation and phytotoxicity in two wild plant species of Almadén area, Chemosphere, 63(11), 1969-1973, DOI: 10.1016/j.chemosphere.2005.09.043, 2006.

Mowat, L. D., St. Louis, V. L., Graydon, J. A., and Lehnherr, I.: Influence of forest canopies on the deposition of methylmercury to boreal ecosystem watersheds, Environ. Sci Technol., 45(12), 5178-5185, DOI: 10.1021/es104377y, 2011.

Nagy, N. E., Sikora, K., Krokene, P., Hietala, A. M., Solheim, H., and Fossdal, C. G.: Using laser micro-dissection and qRT-PCR to analyze cell type-specific gene expression in Norway spruce phloem, PeerJ, 2, e362, DOI: 10.7717/peerj.362, 2014.

Navrátil, T., Šimeček, M., Shanley, J. B., Rohovec, J., Hojdová, M., and Houška, J.: The history of mercury pollution near the Spolana chlor-alkali plant (Neratovice, Czech Republic) as recorded by Scots pine tree rings and other bioindicators, Sci. Total Environ., 586, 1182-1192, DOI: 10.1016/j.scitotenv.2017.02.112, 2017.

Navrátil, T., Nováková, T., Shanley, J. B., Rohovec, J., Matoušková, S., Vaňková, M., and Norton, S. A.: Larch tree rings as a tool for reconstructing 20th century Central European atmospheric mercury trends, Environ. Sci Technol., 52(19), 11060-11068, DOI: 10.1021/acs.est.8b02117, 2018.

Nováková, T., Navrátil, T., Demers, J. D., Roll, M., and Rohovec, J.: Contrasting tree ring Hg records in two conifer species: Multi-site evidence of species-specific radial translocation effects in Scots pine versus European larch, Sci. Total Environ., 762, 144022, DOI: 10.1016/j.scitotenv.2020.144022, 2021.

Nováková T., Navrátil T., Schütze M., Rohovec J., Matoušková Š., Hošek M., Matys Grygar T.: Reconstructing atmospheric Hg levels near the oldest chemical factory in central Europe using a tree ring archive, Environ. Pollut., 304, 119215, DOI: 10.1016/j.envpol.2022.119215, 2022.

Obrist, D., Agnan, Y., Jiskra, M., Olson, C. L., Colegrove, D. P., Hueber, J., Moore, C. W., Sonke, J. E., and

Helmig, D.: Tundra uptake of atmospheric elemental mercury drives Arctic mercury pollution, Nature, 547(7662), 201-204, DOI: 10.1038/nature22997, 2017.

Obrist, D., Kirk, J. L., Zhang, L., Sunderland, E. M., Jiskra, M., and Selin, N. E.: A review of global environmental mercury processes in response to human and natural perturbations: Changes of emissions, climate, and land use, Ambio, 47(2), 116-140, DOI: 10.1007/s13280-017-1004-9, 2018.

Odabasi, M., Tolunay, D., Kara, M., Falay, E. O., Tuna, G., Altiok, H., Dumanoglu, Y., Bayram, A., and Elbir, T.: Investigation of spatial and historical variations of air pollution around an industrial region using trace and macro elements in tree components, Sci. Total Environ., 550, 1010-1021, DOI: 10.1016/j.scitotenv.2016.01.197, 2016.

O'Connor, D., Hou, D., Ok, Y. S., Mulder, J., Duan, L., Wu, Q., Wang, S., Tack, F. M., and Rinklebe, J.: Mercury speciation, transformation, and transportation in soils, atmospheric flux, and implications for risk management: A critical review, Environ. Int., 126, 747-761, DOI: 10.1016/j.envint.2019.03.019, 2019.

Peckham, M. A., Gustin, M. S., Weisberg, P. J., and Weiss-Penzias, P.: Results of a controlled field experiment to assess the use of tree tissue concentrations as bioindicators of air Hg, Biogeochem., 142(2), 265-279, DOI: 10.1007/s10533-018-0533-z, 2019a.

Peckham, M. A., Gustin, M. S., and Weisberg, P. J.: Assessment of the suitability of tree rings as archives of global and regional atmospheric mercury pollution, Environ. Sci Technol., 53(7), 3663-3671, DOI: 10.1021/acs.est.8b06786, 2019b.

Peralta-Videa, J. R., Lopez, M. L., Narayan, M., Saupe, G., and Gardea-Torresdey, J.: The biochemistry of environmental heavy metal uptake by plants: implications for the food chain, Int. J. Biochem. Cell Biol., 41(8-9), 1665-1677, DOI: 10.1016/j.biocel.2009.03.005, 2009.

Pfautsch, S., Hölttä, T., and Mencuccini, M.: Hydraulic functioning of tree stems—fusing ray anatomy, radial transfer and capacitance, Tree Physiol., 35(7), 706-722, DOI: 10.1093/treephys/tpv058, 2015.

Rea, A. W., Lindberg, S. E., and Keeler, G. J.: Assessment of dry deposition and foliar leaching of mercury and selected trace elements based on washed foliar and surrogate surfaces. Environ. Sci Technol., 34(12), 2418-2425, DOI: 10.1021/es991305k, 2000.

Rea, A. W., Lindberg, S. E., and Keeler, G. J.: Dry deposition and foliar leaching of mercury and selected trace elements in deciduous forest throughfall. Atmos. Environ., 35(20), 3453-3462, DOI: 10.1016/S1352-2310(01)00133-9, 2001.

Rea, A. W., Lindberg, S. E., Scherbatskoy, T., and Keeler, G. J.: Mercury accumulation in foliage over time in two northern mixed-hardwood forests. Water Air Soil Pollut., 133(1), 49-67, DOI: 10.1023/A:1012919731598, 2002.

Richard, J. H., Bischoff, C., Ahrens, C. G., and Biester, H.: Mercury (II) reduction and co-precipitation of metallic mercury on hydrous ferric oxide in contaminated groundwater, Sci. Total Environ., 539, 36-44, DOI: 10.1016/j.scitotenv.2015.08.116, 2016.

Scanlon, T. M., Riscassi, A. L., Demers, J. D., Camper, T. D., Lee, T. R., and Druckenbrod, D. L.: Mercury accumulation in tree rings: observed trends in quantity and isotopic composition in Shenandoah National Park, Virginia, J. Geophys. Res. Biogeosci., 125(2), p.e2019JG005445, DOI: 10.1029/2019JG005445, 2020.

Schrenk, V., and Hiester, U.: Analysis of Subsurface Remediation Technologies for Brownfield Redevelopments, REVIT: revitalising industrial sites, City of Stuttgart, Stuttgart, Germany, P042/0702, 97. https://www.researchgate.net/publication/283082200_Analysis_of_Subsurface

_Remediation_Technologies_for_Brownfield_Redevelopments, 2007.

Schroeder, W. H., and Munthe, J.: Atmospheric mercury—an overview. Atmos. Environ., 32(5), 809-822, DOI: 10.1016/S1352-2310(97)00293-8, 1998.

Selin, N. E.: Global biogeochemical cycling of mercury: a review, Annu. Rev. Environ. Resour., 34, 43-63, DOI: 10.1146/annurev.environ.051308.084314, 2009.

Selin, N. E., Jacob, D. J., Yantosca, R. M., Strode, S., Jaeglé, L., and Sunderland, E. M.: Global 3-D land-ocean-atmosphere model for mercury: Present-day versus preindustrial cycles and anthropogenic enrichment factors for deposition, Global Biogeochem. Cy., 22(2), GB2011, DOI: 10.1029/2007GB003040, 2008.

Siwik, E. I., Campbell, L. M., and Mierle, G.: Distribution and trends of mercury in deciduous tree cores, Environ. Pollut., 158(6), 2067-2073, DOI: 10.1016/j.envpol.2010.03.002, 2010.

Sprovieri, F., Pirrone, N., Bencardino, M., D'Amore, F., Carbone, F., Cinnirella, S., Mannarino, V., Landis, M., Ebinghaus, R., Weigelt, A., Brunke, E.G., Labuschagne, C., Martin, L., Munthe, J., Wängberg, I., Artaxo, P., Morais, F., de Melo Jorge Barbosa, H., Brito, J., Cairns, W., Barbante, C., del Carmen Diéguez, M., Garcia P. E., Dommergue, A., Angot, H., Magand, O., Skov, H., Horvat, M., Kotnik, J., Read, K. A., Mendes Neves, L., Gawlik, B. M., Sena, F., Mashyanov, N., Obolkin, V., Wip, D., Feng, X. B., Zhang, H., Fu, X., Ramachandran, R., Cossa, D., Knoery, J., Marusczak, N., Nerentorp, M., and Norstrom C.: Atmospheric mercury concentrations observed at ground-based monitoring sites globally distributed in the framework of the GMOS network, Atmos. Chem. Phys., 16(18), 11915-11935, DOI: 10.5194/acp-16-11915-2016, 2016.

Sun, R., Streets, D. G., Horowitz, H. M., Amos, H. M., Liu, G., Perrot, V., Toutain, J. P., Hintelmann, H., Sunderland, E. M., Sonke, J. E., and Blum, J. D.: Historical (1850–2010) mercury stable isotope inventory from anthropogenic sources to the atmosphere. Elementa Sci. Anthropocene, 2016, 4, 91.

Szponar, N., McLagan, D. S., Kaplan, R. J., Mitchell, C. P., Wania, F., Steffen, A., Stupple, G. W., Monaci, F., and Bergquist, B. A.: Isotopic characterization of atmospheric gaseous elemental mercury by passive air sampling, Environ. Sci Technol., 54(17), 10533-10543, DOI: 10.12952/journal.elementa.000091, 2020.

Taylor, A. M., Gartner, B. L., and Morrell, J. J.: Heartwood formation and natural durability-a review. Wood Fibre Sci., 2002, 34(4), 587-611.

Wang, X., Luo, J., Yin, R., Yuan, W., Lin, C.J., Sommar, J., Feng, X., Wang, H., and Lin, C.: Using mercury isotopes to understand mercury accumulation in the montane forest floor of the Eastern Tibetan Plateau. Environ. Sci Technol., 2017, 51(2), 801-809.

Wang, X., Yuan, W., Lin, C. J., Luo, J., Wang, F., Feng, X., Fu, X., and Liu, C.: Underestimated sink of atmospheric mercury in a deglaciated forest chronosequence, Environ. Sci Technol., 54(13), 8083-8093, DOI: 10.1021/acs.est.0c01667, 2020.

Wang, X., Yuan, W., Lin, C. J., Wu, F., and Feng, X.: Stable mercury isotopes stored in Masson Pinus tree rings as atmospheric mercury archives, J. Hazard. Mater., 415, 125678, DOI: 10.1016/j.jhazmat.2021.125678, 2021.

Weis, R.: Vor 100 Jahren brannte in Titisee-Neustadt das Dampfsäge- und Holzwerk Himmelsbach, *Badische Zeitung BZ*, https://www.badische-zeitung.de/vor-100-jahren-brannte-in-titisee-neustadt-das-dampfsaege-und-holzwerk-himmelsbach--188906523.html, 2020.

Wiederhold, J. G., Christopher J. C., Daniel, K., Infante, I., Bourdon D., and Kretzschmar, R.: Equilibrium Mercury Isotope Fractionation between Dissolved Hg(II) Species and Thiol-Bound Hg, Environ. Sci. Technol., 44(11), 4191–4197, DOI:10.1021/es100205t, 2010.

Wohlgemuth, L., Osterwalder, S., Joseph, C., Kahmen, A., Hoch, G., Alewell, C., and Jiskra, M.: A bottom-up quantification of foliar mercury uptake fluxes across Europe, Biogeosci., 17(24), 6441-6456, DOI: 10.5194/bg-17-6441-2020, 2020.

Wright, G., Woodward, C., Peri, L., Weisberg, P. J., and Gustin, M. S.: Application of tree rings [dendrochemistry] for detecting historical trends in air Hg concentrations across multiple scales. Biogeochem., 120(1), 149-162, DOI: 10.1007/s10533-014-9987-9, 2014.

Yamakawa, A., Amouroux, D., Tessier, E., Bérail, S., Fettig, I., Barre, J.P., Koschorreck, J., Rüdel, H., and Donard, O.F.: Hg isotopic composition of one-year-old spruce shoots: Application to long-term Hg atmospheric monitoring in Germany, Chemosphere, 279, 130631, DOI: 10.1016/j.chemosphere.2021.130631, 2021.

Yanai, R. D., Yang, Y., Wild, A. D., Smith, K. T., and Driscoll, C. T.: New Approaches to Understand Mercury in Trees: Radial and Longitudinal Patterns of Mercury in Tree Rings and Genetic Control of Mercury in Maple Sap, Water Air Soil Pollut., 231, 1-10, DOI: 10.1007/s11270-020-04601-2, 2020.

York, D., Evensen, N. M., Martınez, M. L., and De Basabe Delgado, J.: Unified equations for the slope, intercept, and standard errors of the best straight line, Am. J. Phys., 72(3), 367-375, DOI: 10.1119/1.1632486, 2004.

Yuan, W., Sommar, J., Lin, C. J., Wang, X., Li, K., Liu, Y., Zhang, H., Lu, Z., Wu, C., and Feng, X.: Stable isotope evidence shows re-emission of elemental mercury vapor occurring after reductive loss from foliage, Environ. Sci Technol., 53(2), 651-660, DOI: 10.1021/acs.est.8b04865, 2018.

Zhang, L., Wright, L. P., and Blanchard, P.: A review of current knowledge concerning dry deposition of atmospheric mercury, Atmos. Environ., 43(37), 5853-5864, DOI: 10.1016/j.atmosenv.2009.08.019, 2009.

Zheng, W., and Hintelmann, H.: Mercury isotope fractionation during photoreduction in natural water is controlled by its Hg/DOC ratio, Geochim. Cosmochim. Acta, 73(22), 6704-6715, DOI: 10.1016/j.gca.2009.08.016, 2009.

Zhou, J., Wang, Z., Zhang, X., and Gao, Y.: Mercury concentrations and pools in four adjacent coniferous and deciduous upland forests in Beijing, China, J. Geophys. Res. Biogeosci., 122(5), 1260-1274, DOI: 10.1002/2017JG003776, 2017.

Zhou, J., Obrist, D., Dastoor, A., Jiskra, M. and Ryjkov, A.: Vegetation uptake of mercury and impacts on global cycling. *Nature Reviews Earth & Environment*, *2*(4), 269-284, DOI: 10.1038/s43017-021-00146-y, 2021.

791
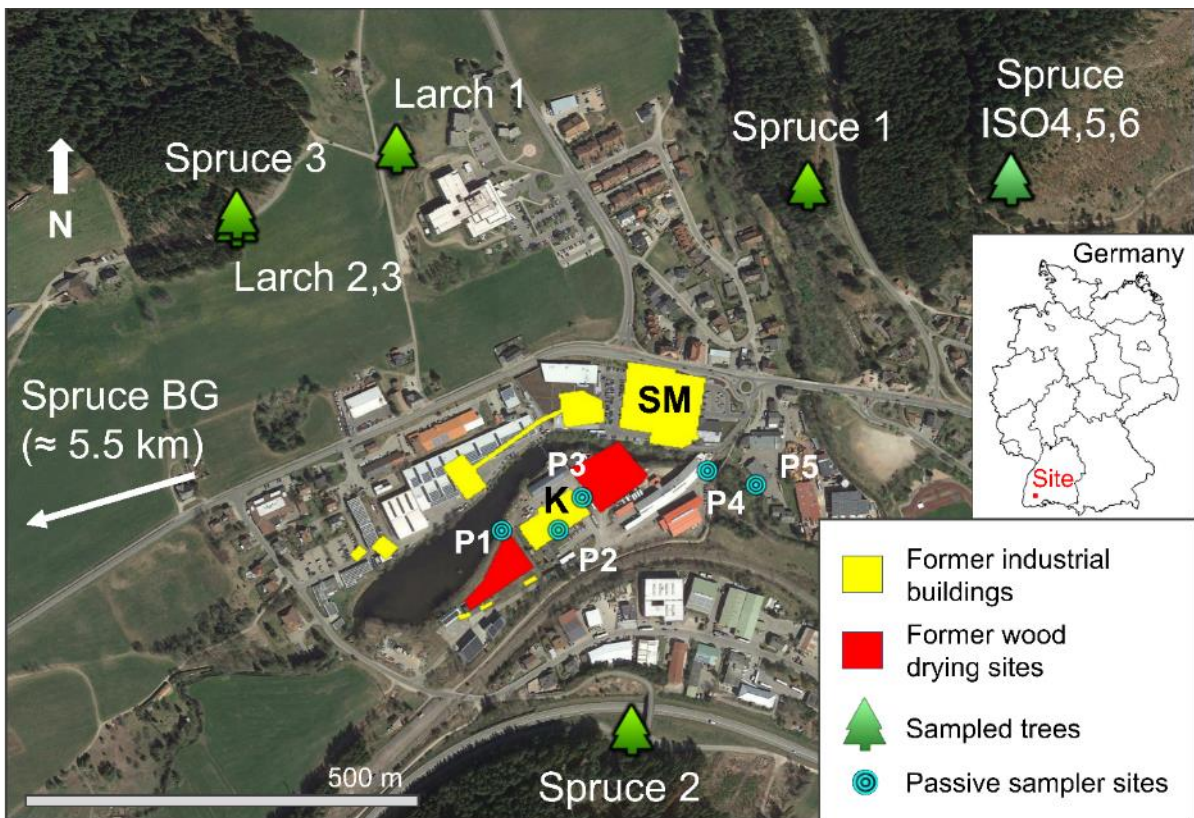
Figure 1: Map showing the location of sampled trees, former industrial buildings and wood drying sites
(before 1968), and passive sampler locations (labelled P1—P5). The location of Spruce background tree
(Spruce BG) is ≈5.5 kilometres west southwest of the study site (direction indicated on map). SM – Former
sawmill; K – former kyanisation hall/wood treatment area. The three Spruce ISO trees are from the
deforested stand in the northwest of Fig. 1; exact location of each of these trees within this stand is unknown
(trees felled by forest workers). ©Google Earth 2019.

798
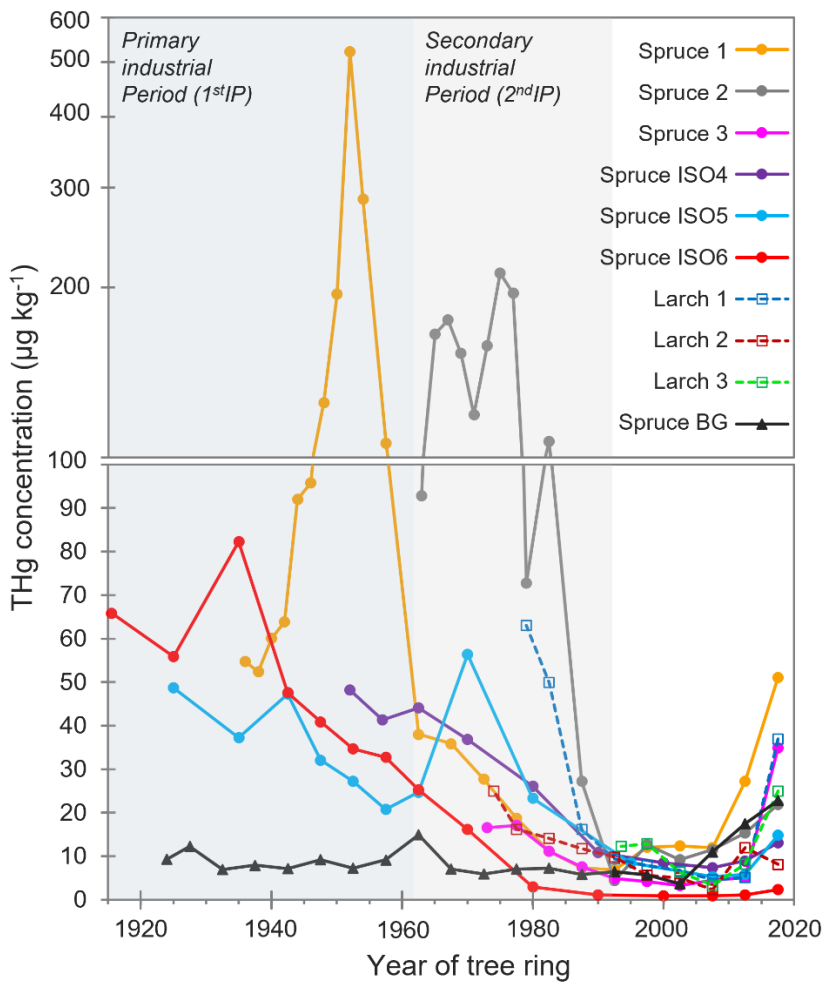
799

800 ***Figure 2***: *THg concentrations in tree rings dated by year. Years of tree rings correspond to the middle*
801 *point of samples of combined adjacent rings (i.e., 0—5 year = 2.5 years). Y-axis is split at 100 µg·kg-1*
802 *changing from normal- to log-scale due to the very high concentrations measured in Spruce 1 and Spruce 2.*
803 *1ˢᵗIP (before 1962) and 2ⁿᵈIP (1962—1992) are highlighted.*

804

805
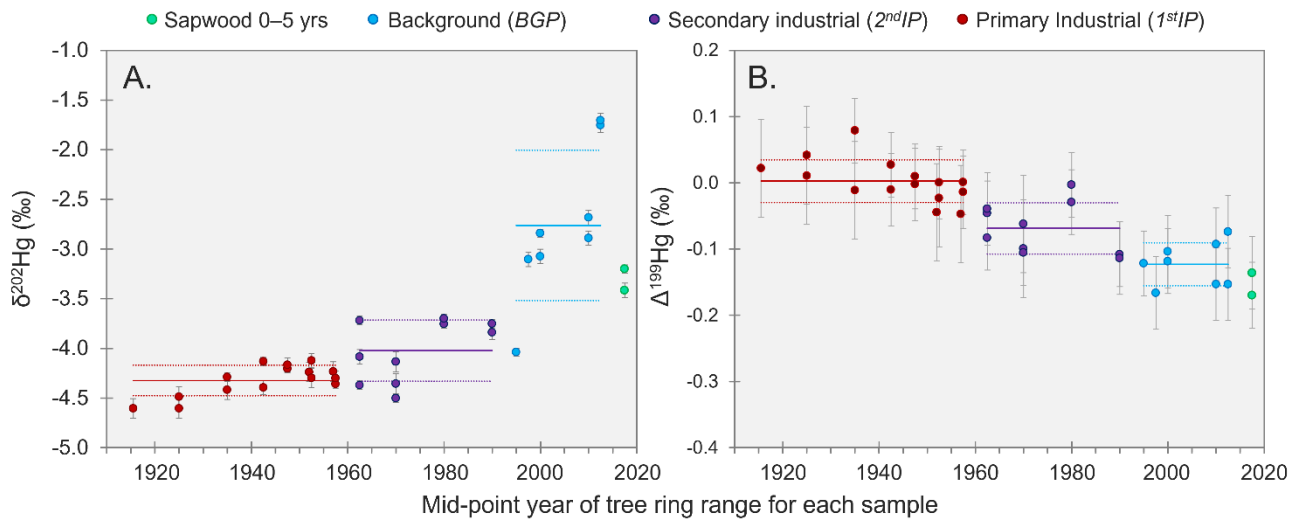
Figure 3: $\delta^{202}Hg$ *(Panel A) and $\Delta^{199}Hg$ (Panel B) in tree rings dated by year for samples from Spruce ISO4—6 trees. Solid and dotted lines for each period represent the mean and standard deviation, respectively. Data displayed are the composite of all three trees (figures for individual trees are shown in Section S6). Data for THg plotted against MDF and THg against MIF are shown in Section S7. Error bars for individual datapoints represent session 2SD for secondary standard "ETH Fluka".*

806
807
808
809
810
811

812
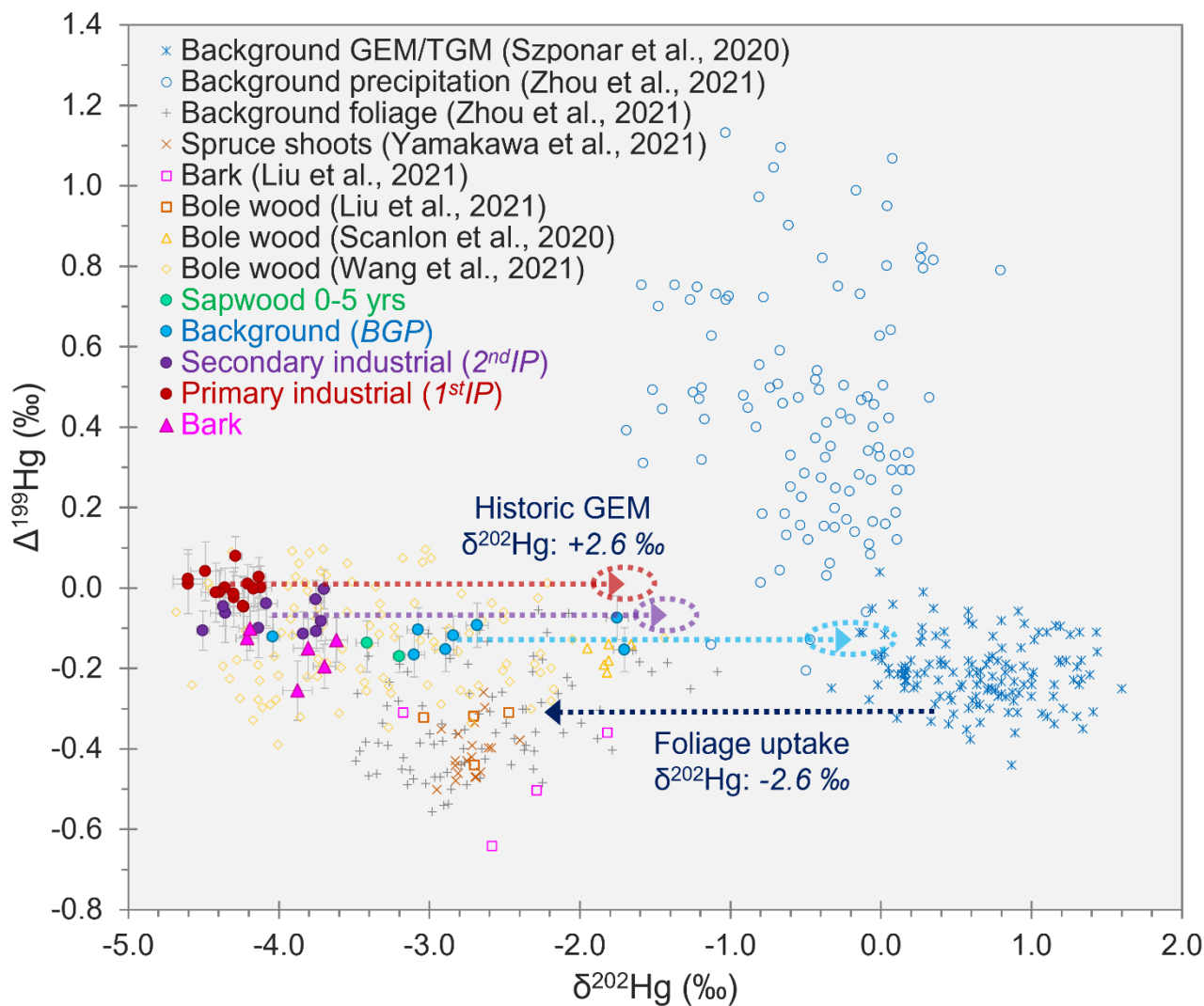
Figure 4: *Relationships between $\Delta^{199}Hg$ and $\delta^{202}Hg$ for tree rings samples from Spruce ISO4—6 trees analysed for Hg stable isotopes (data with solid markers). Figure includes the $\Delta^{199}Hg$ and $\delta^{202}Hg$ values for tree samples (bole wood, bark, foliage, and shoots) from other studies. Additionally, background TGM/GEM data were included to show the $\approx$-2.6 ‰ MDF associated with stomatal uptake of GEM (dark blue dotted line), and background precipitation samples were included to demonstrate that there was little influence from precipitation on found Hg in within trees. The red, purple, and light-blue dotted lines indicate the predicted GEM values in air at the site during the $1^{st}IP$, $2^{nd}IP$, and BGP, respectively, based off the mean measured $\delta^{202}Hg$ values in tree rings for these respective periods (MIF was assumed to be zero for stomatal uptake in these calculations).*

822